Journal of Neurocytology **13**, 639–664 (1984)

Stellate neurons in rat dorsal cochlear nucleus studied with combined Golgi impregnation and electron microscopy: synaptic connections and mutual coupling by gap junctions

F. G. WOUTERLOOD[1]*, E. MUGNAINI[1]†, K. K. OSEN[2] and A.-L. DAHL[1]

[1]*Laboratory of Neuromorphology, Department of Biobehavioral Sciences, The University of Connecticut, Storrs, Connecticut 06268, USA*
[2]*Institute of Anatomy, University of Oslo Medical School, Karl Johansgate 47, Oslo 1, Norway*

Received 3 January 1984; revised 5 March 1984; accepted 19 March 1984

Summary

Stellate neurons in the outer two layers of the rat dorsal cochlear nucleus (DCN) were studied by the Golgi–EM method. Stellate cell bodies are usually spherical or ovoidal and range from 9 μm to 14 μm in mean diameter. The smallest cells are situated underneath the ependymal layer and the largest cells in layer 2. Primary dendrites are short, thin and smooth and arise abruptly from the perikaryon, without a tapering main stem. Meandering secondary and tertiary dendrites extend in all directions, carry few pleomorphic spines lacking a spine apparatus and often show artifactual beading. The axons are impregnated only for a short distance (10–45 μm). The nucleus is indented, the nucleolus varies in position, and the chromatin, evenly dispersed in the centre, forms small clumps along the nuclear envelope. The cytoplasm is rich in free polyribosomes and contains scattered cisterns of granular endoplasmic reticulum. Varicosities of thin fibres, containing round synaptic vesicles, form asymmetric synapses on perikarya, dendritic shafts and spines of stellate cells. Such fibres run parallel to the long axis of the DCN or are oriented radially and are interpreted as axons of cochlear granule cells. Two kinds of bouton containing pleomorphic vesicles, one kind electron lucent and the other electron dense, form symmetric synapses on perikarya and dendritic shafts of stellate cells. The lucent boutons occur more frequently than the dense boutons, especially on the distal dendritic branches. The boutons with pleomorphic vesicles presumably represent terminals of local circuit neurons, probably the stellate and cartwheel cells.

In addition, stellate cells show numerous dendro-somatic and dendro-dendritic appositions characterized by gap junctions and puncta adhaerentia. Most of the dendrites involved in these

**Present address:* Department of Anatomy, Vrije Universiteit, P.O. Box 7161, 1007 MC Amsterdam, The Netherlands.

†To whom requests for reprints should be sent.

0300-4864/84 $03.00 + .12

appositions resemble stellate cell dendrites and it is concluded that DCN stellate cells are coupled electrotonically with one another. The axons of stellate cells acquire a thin myelin sheath. Since the Golgi impregnation did not stain axons of stellate cells past this point, we were unable to demonstrate the synaptic targets of stellate cells.

Introduction

The mammalian acoustic tubercle, or dorsal cochlear nucleus (DCN), is a laminated brain stem region situated in the floor of the lateral recess of the fourth ventricle caudal and lateral to the inferior cerebellar peduncle. In the outer two layers of the DCN, five major classes of neuron have been distinguished: pyramidal (also known as fusiform, bipolar or principal), granule, Golgi, cartwheel and stellate cells (Brawer *et al.*, 1974; Disterhoft *et al.*, 1980; Mugnaini *et al.*, 1980a, b; Lorente de Nó, 1981a; Osen & Mugnaini, 1981; Browner & Baruch, 1982; Webster & Trune, 1982; Rhode *et al.*, 1983; Wouterlood & Mugnaini, 1984). It has been demonstrated that pyramidal neurons project to the central nucleus of the contralateral inferior colliculus (reviewed by Brodal, 1981; Willard & Ryugo, 1983; Blackstad *et al.*, 1984). The other four cell classes represent various types of interneuron.

Although cochlear stellate cells have been identified in several mammalian species, their role in the neuronal circuitry of the DCN remains obscure (Osen & Mugnaini, 1981). While the main ultrastructural and synaptic features of pyramidal (Kane, 1974a), granule (Mugnaini *et al.*, 1980b), Golgi (Mugnaini *et al.*, 1980b) and cartwheel cells (Wouterlood & Mugnaini, 1984) have been investigated, the characterization of stellate cell bodies and processes at the ultrastructural level has not been resolved satisfactorily. By electron microscopy of serial sections of Golgi-impregnated stellate cells from the DCN of adult rats, treated either according to the gold substitution procedure of Fairén *et al.* (1977, 1981) or with a photographic developer (Wouterlood *et al.*, 1983), we have established a set of criteria for their identification in standard thin sections. Although the synaptic targets of stellate cells remain to be demonstrated, our study indicates that DCN stellate cells share several fine structural and synaptic features with cerebellar stellate cells, and may exert analogous functions.

Materials and methods

This study is based on seven two-month-old female Wistar rats (200 g) for Golgi–EM and on 12 Wistar rats of either sex weighing 240–400 g for standard electron microscopy. Under sodium pentobarbital anaesthesia, the animals were perfused with 100 ml of calcium-free Ringer solution (pH 7.3, 37° C, delivery pressure 110 cm H_2O) followed by 500 ml of 1% formaldehyde and 1.25% glutaraldehyde in 0.12 M phosphate buffer (pH 7.3, 37° C) and subsequently by 500 ml of 3% glutaraldehyde in the same buffer at room temperature (Friedrich & Mugnaini, 1981). Several hours after the aldehyde perfusion, the brains were dissected and the cerebella removed to expose the cochlear nuclei. For Golgi–EM, 4 mm thick slabs of the brain stem containing the DCN were impregnated by a variant of the del Rio-Hortega modification of the Golgi–Kopsch procedure (Adams, 1979; Mugnaini *et al.*, 1980b). After treatment in mordant (4% formaldehyde, 2.5%

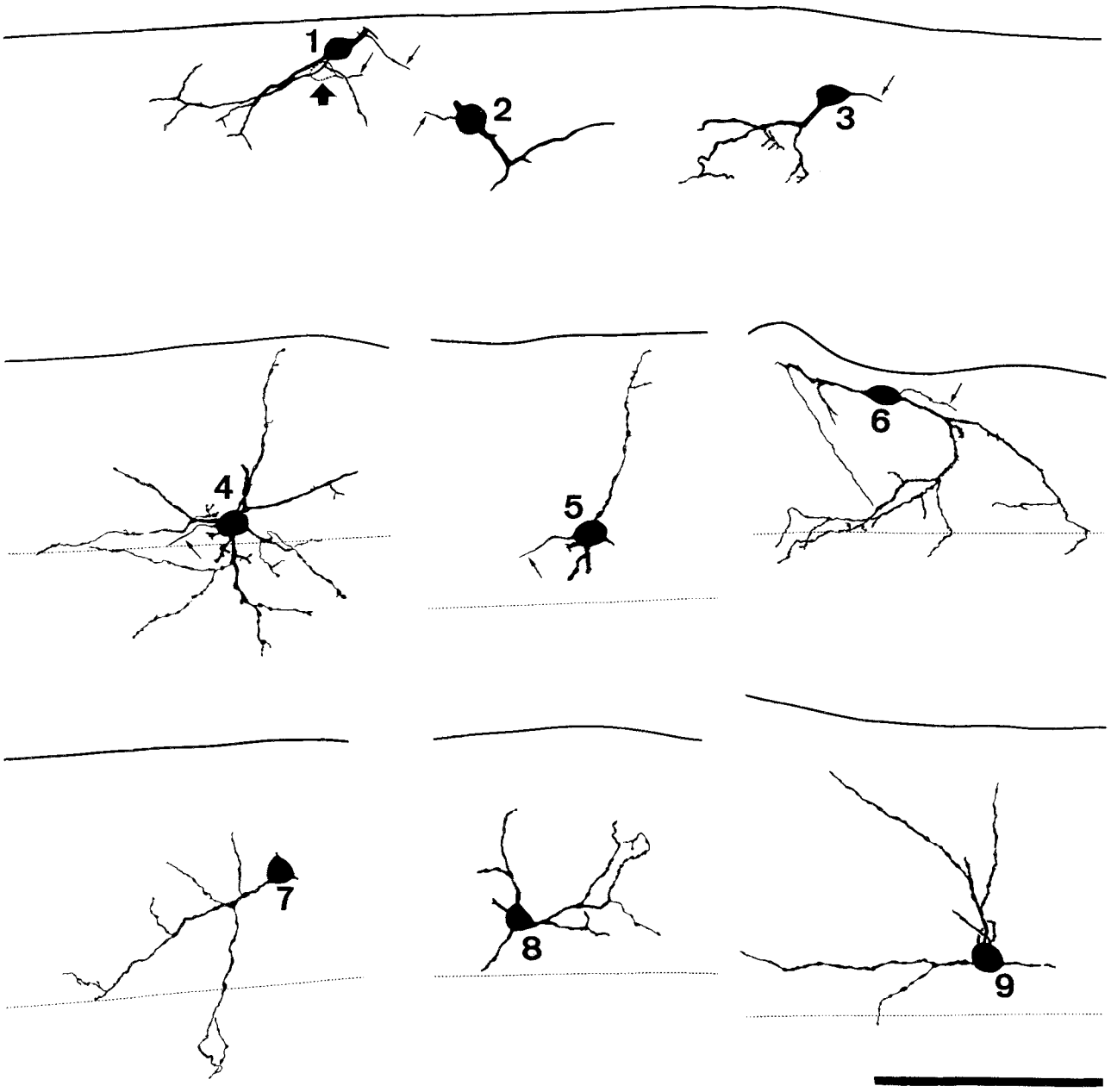

Fig. 1. Camera lucida drawings of the stellate cells examined by electron microscopy. Cells no. 1 2, and 3 are drawn in their original location in the same Vibratome section; the other cells are from different sections and different areas. Cell no. 1 is accompanied by a very weakly impregnated stellate cell (not numbered, indicated by large arrow). Small arrows indicate axons of the stellate cells. The axons of cells, no. 1, 4, 5 and 6 and the 'ghost' cell were traced in serial ultrathin sections. Continuous lines indicate ependymal surfaces and dotted lines the border between layers 1 and 2. Scale bar: 100 μm.

potassium dichromate and 1% chloral hydrate) for 3–4 days at room temperature and in the dark, the slabs were rinsed quickly in distilled water, covered by a thin layer of 2% agar to prevent growth of silver chromate crystals on the ependymal surface of the DCN, and put in 0.75% silver nitrate for 2–3 days (room temperature, in the dark). The slabs were then embedded in 5% agar and sliced at 60–80 μm on a Vibratome (Oxford Instruments, USA), in a chilled bath fluid consisting of 50% ethanol saturated with silver chromate.

Slices in which stellate cells appeared well impregnated were transferred to glass vials containing bath fluid and processed either by the gold substitution procedure (Fairén *et al.*, 1977, 1981) or treated with Kodalith (Eastman Kodak Co., Rochester, New York, USA) according to Wouterlood *et al.* (1983). After either treatment, the slices were stored in cold 0.1 M cacodylate buffer, pH 7.3, until further processing. This involved postfixation in 2% buffered osmium tetroxide, *en bloc* staining in 2% aqueous uranyl acetate, dehydration and embedding in mixtures of TAAB resin and Epon 812. During thin sectioning the specimen holder with the mounted block was taken out of the ultramicrotome at regular intervals, inserted on a modified microscope stage and observed in a light microscope fitted with a drawing tube and a camera (Wouterlood, 1979). In this way, the stellate cells were thin sectioned serially while they could be observed, drawn and photographed (micrographs not shown) at any stage of sectioning, without the need for semithin sectioning. Serial sections were collected on Formvar-coated slot grids. Nine solitarily impregnated cells (Fig. 1) were selected for analysis in the electron microscope.

For standard electron microscopy, the DCN was cut under a dissection microscope into 1 mm thick slices either parallel or transverse to its long axis. The slices were postfixed in 2% buffered osmium tetroxide, rinsed in buffer, treated *en bloc* with 2% maleate-buffered uranyl acetate and embedded in Epon 812. Short series of ultrathin sections were collected on Formvar-coated slot grids or on naked 400 mesh grids. All sections were stained with uranyl acetate and lead citrate, and were examined in a Zeiss EM-10 electron microscope.

Results

General features of the rat DCN

As in other nonprimate mammals (Lorente de Nó, 1981a) the rat DCN contains the following strata: a superficial layer (1, or molecular layer); a cell-rich layer (2, or pyramidal cell layer); and a deeper region with numerous myelinated axons and scattered neurons corresponding to layers 3–4 and the central nucleus in other mammals. Layer 1 is superificially covered by ependyma, whereas deeply it is only indistinctly limited by the second layer. The molecular layer consists of dendritic profiles running in all directions, thin, predominantly unmyelinated fibres that course parallel to each other and to the long axis of the DCN, and a loose network of myelinated fibres particularly prominent at the border with layer 2. Scattered among these elements are the cell bodies of granule cells and other small neuronal types. An estimation of the relative frequency of cells of the various neuronal classes in layers 1 and 2 of rat DCN has been published recently (Wouterlood & Mugnaini, 1984).

Light microscopy of Golgi-impregnated stellate cells

Stellate cells occur in layers 1 and 2. The large majority of them have spherical or ovoidal cell bodies. Stellate cells with fusiform cell bodies occur occasionally (cell no. 6 of Fig. 1).

The cell bodies range in mean diameter from 9 μm to 14 μm and have primary dendrite emanating in all directions, commonly without a tapering base (Fig. 1). The perikarya of stellate cells in the subependymal portion of layer 1 generally have smaller diameters than those located deeper in layer 1 and in layer 2. The smooth primary dendrites are usually short (10–30 μm) and have a uniform diameter (approximately 1 μm). They usually branch dichotomously or give rise to side branches at wide angles. The branching points may appear slightly enlarged. The secondary dendrites carry a few pleomorphic spines definable as sessile knobs, gemmules and small bulbs with short stalks. The third order dendrites generally are very thin (0.5 μm) and often have a beaded appearance which we regard as an artifact (*état moniliforme*; Cajal, 1911). Some of the tertiary dendrites carry no distinct spines and end in tapered or blunt tips. Stellate cell dendrites extend in all directions and appear meandering when viewed at high magnification. The dendritic fields span 100–150 μm in diameter. As we used relatively thin sections (60–80 μm), the dendritic trees of all cells appear incomplete (Fig. 1). In this study, no attemps were made to follow individual dendrites in successive Golgi sections. Dendrites of stellate cells located in layer 1 may penetrate layer 2; some dendrites of layer 2 stellate cells may enter layer 3. Stellate cells in layer 2 invariably show some dendrites extending into layer 1.

In our sample, layer 2 stellate cells were not solitarily impregnated. Therefore, only layer 1 stellate cells were used for Golgi–EM. Two of those cells (nos. 4 and 7) have well-impregnated dendrites extending in layer 2. The axons of stellate cells are very thin (0.5 μm diameter) and originate from the cell body or from a primary dendrite. The axons are impregnated for a short distance (10–45 μm). Collaterals are not formed by the initial portions of the axons visualized in our material.

Electron microscopy of Golgi-impregnated stellate cells

The cell bodies of the sampled, Golgi-impregnated stellate cells (Figs. 2, 3, 13, 14) have smooth contours and their mean diameters (9–14 μm) match the range of the general population. The nucleus, which always occupies a large portion of the cell soma, is conspicuously indented and the chromatin, evenly dispersed in the centre, forms small clumps along the nuclear envelope. Larger clumps of heterochromatin often occur at the bases of the nuclear indentations. The position of the nucleolus ranges from central to peripheral. The cytoplasm contains individual cisterns of granular endoplasmic reticulum of varying length, but stacks of several granular cisterns are rare. Particularly numerous free polyribosomes are seen where the cytoplasm is most abundant and within the indentations of the nuclear perimeter. The Golgi apparatus is usually confined to the region of the cell body most rich in cytoplasm. Mitochondria with diameters ranging between 0.2 and 0.3 μm are dispersed throughout the cytoplasm, but are absent in the nuclear indentations. Subsurface cisterns are common. In two cells only, we encountered one subsurface cistern associated with a mitochondrion (SCM-complex).

All stellate cells have few axo-somatic synapses. The number of axo-somatic terminals

is usually higher in the larger cells. Two main categories can be distinguished among axo-somatic terminals: a category of boutons forming symmetrical synaptic junctions (Colonnier, 1968; type II of Gray, 1959) and provided with pleomorphic synaptic vesicles, and a second category of boutons forming asymmetrical synaptic junctions (type I of Gray, 1959) and provided with round synaptic vesicles. The two main categories of bouton occur with approximately equal frequency. The first category of terminals comprises two kinds of bouton, here referred to as PVL and PVD bountons. PVL (pleomorphic vesicles, lucent) boutons range in size from 0.3 to 2.0 μm, have an electron-lucent axoplasm and form single, small junctional complexes (Fig. 6). They usually contain one or two mitochondria of the same size or larger than stellate perikaryal mitochondira. Occasionally, PVL terminals contain a bundle of neurofilaments. PVL boutons occur more frequently than PVD boutons. PVD (pleomorphic vesicles, dense) boutons display a flocculent axoplasm; they range in size from 0.3 to 3.0 μm, and are packed with a large number of flattened to oval synaptic vesicles. PVD terminals frequently form a single, long (up to 1.0 μm), synaptic junction or multiple, small synapses (Figs. 4, 6). PVD terminals contain 1–6 mitochondira of the same size or occasionally larger than stellate perikaryal mitochondira. A few axo-somatic boutons with pleomorphic vesicles and symmetric synapses cannot be classified confidently in either subcategory. The second category of axo-somatic terminals, referred to as RV (round vesicles) boutons are small to medium size (0.3–1.5 μm) and have an electron-lucent matrix (Fig. 7). They represent varicosities of thin fibres orientated either radially or parallel to the long axis of the DCN.

In addition to axo-somatic appositions, the stellate cell bodies are also involved in dendro-somatic appositions (3–6 per whole cell body). These contacts are formed by dendritic profiles usually less than 1 μm in diameter (Figs. 2, 3). The dendro-somatic appositions show two types of specialized cell junctions classified as gap junctions and puncta adhaerentia according to widely recognized criteria (Peters *et al.*, 1976). Gap junctions vary in length between 80 and 500 nm. They appear as closely apposed, parallel plasma membranes, in register with symmetric cytoplasmic plates of electron-dense material. The intercellular cleft measures less than 2 nm and is occluded

---

Fig. 2. Cell body (SC_1) and primary dendrite of the subependymally located stellate cell no. 1. Note the smooth cell contour and relatively large, indented nucleus. The impregnated cell (SC_2) deep to cell no. 1 is the 'ghost' cell of Fig. 1, sectioned through its axon hillock and intitial axon segment. This cell displayed all characteristics typical of stellate cells. Arrows indicate the sites at which two dendro-dendritic junctions (solid arrows) and a dendro-axonic junction (open arrow) were observed at higher magnification. The initial axon segment of SC_2 was traced further; it acquired a myelin sheath and lost impregnation. Gold substitution. × 4900.

Fig. 3. Cell body (SC) of stellate cell no. 7. Note the nuclear indentations, the eccentric nucleolus, the absence of large assemblies of cisterns of granular ER, and the high nucleus to cytoplasm ratio. A dendro-somatic apposition is indicated by open arrow. Inside the lucent profile labelled PVL pleomorphic synaptic vesicles were seen at higher magnifications. Portion of a cartwheel neuron (CN) is included in the picture. Gold substitution. × 11 200.

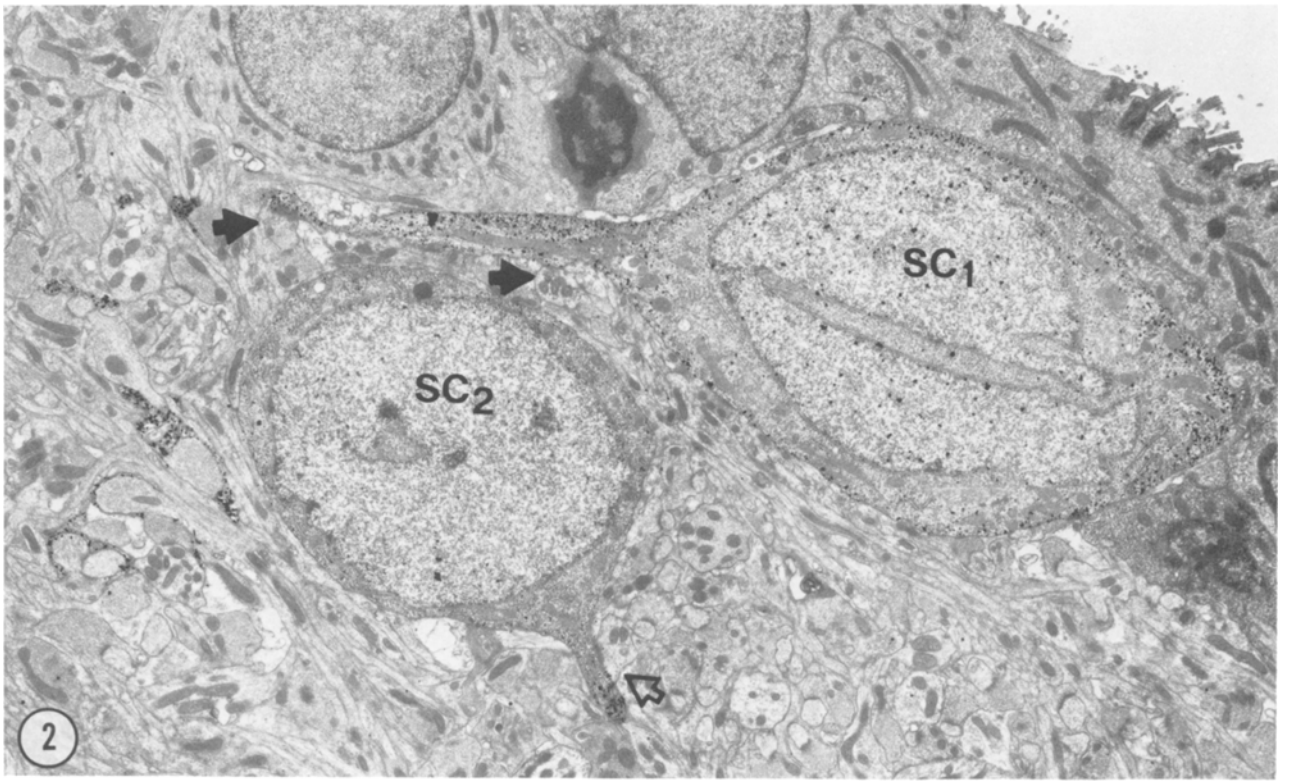
SC1
SC2
2

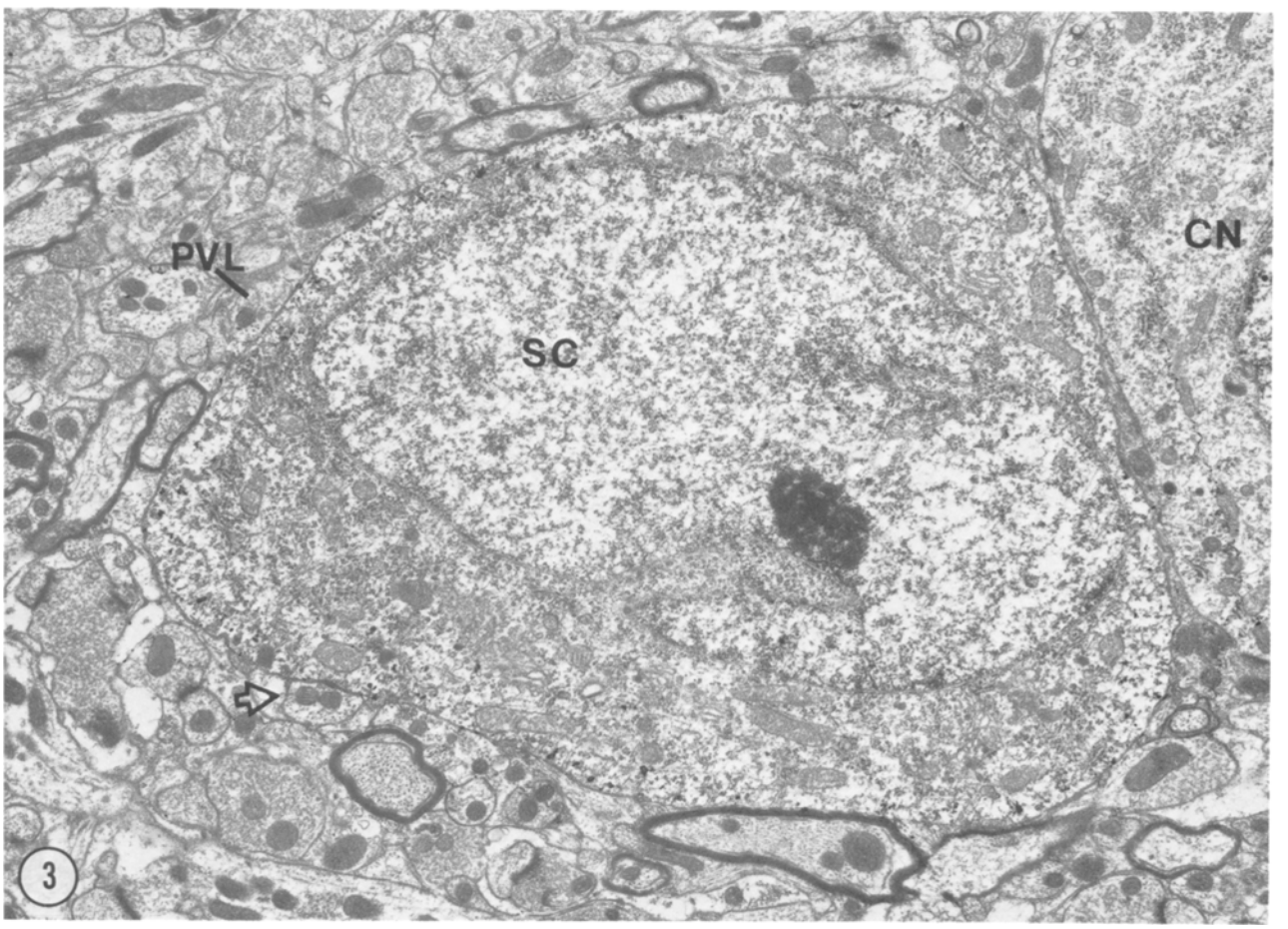
PVL
SC
CN
3

at points. Puncta adhaerentia appear as small (0.2 μm) spots of increased plasma membrane and cytoplasmic densities. The intercellular gap widens to 20 nm. The cytoplasmic plaques of dense material are usually symmetric, but appear sometimes slightly thicker on the dendritic side than on the somatic side of the junction. The most common type of dendro-somatic apposition consists of a gap junction flanked by one or two puncta adhaerentia (Figs. 4–6). It must be noted here that the dendritic profiles which are engaged in the dendro-somatic contacts show the same size and morphological characteristics as secondary stellate dendrites.

Primary dendrites, which arise abruptly from the cell bodies, are thin (1.0–1.2 μm) and smooth, and contain a few polyribosomes, microtubules, saccules of the endoplasmic reticulum, and scattered mitochondria. Often, small elevations are present in the dendritic contour on which either axon terminals make synaptic contact, or dendro-dendritic appositions featuring a gap junction and puncta adhaerentia occur (Figs. 8, 9, 12). The same classes of axon terminals seen on the soma contact also the shafts of primary dendrites. PVD terminals, which are infrequently seen on the perikaryon, decrease in number further along the primary dendrites and are usually absent on secondary dendrites.

Secondary and tertiary dendrites are contacted by PVL and RV terminals (Fig. 11), and in addition form frequent contacts with thin, dendritic profiles that display the same fine structural characteristics as stellate cell dendrites. Invariably the dendro-dendritic appositions include puncta adhaerentia, either solitarily or in combination with a gap junction. Examination of serial sections shows that there is at least one gap junction per 10 μm of dendritic length. The spines of stellate cell dendrites are contacted by RV terminals (Fig. 10). Most of these spines are filled with flocculent material only; they do not show a membranous spine apparatus, unlike the spines of cartwheel cell dendrites (Wouterlood & Mugnaini, 1984).

The axon emerges from the cell body without an axon hillock (Figs. 13, 14). These axons were well impregnated, and thus easily traced in serial thin sections in four of the

---

Fig. 4. Detail of the cell body of stellate cell no. 5 with apposed boutons (RV and PVD) and dendrite (D). The dendro-somatic apposition involves a punctum adhaerens (solid arrow). Of the two boutons, one contains round synaptic vesicles (RV) and the other pleomorphic vesicles and a dense matrix (PVD). Kodalith treatment. × 38 000.

Fig. 5. Junctional apposition between a nonimpregnated small dendrite (D) and the soma (SC) of stellate cell no. 5. A gap junction (between open arrows) is flanked by two puncta adhaerentia (solid arrows). Kodalith treatment. × 142 000.

Fig. 6. Small dendrite (D) forms two puncta adhaerentia (solid arrows) with the soma (SC) of stellate cell no. 7. The dendrite forms symmetric synapses (open arrows) with PVL and PVD boutons. The PVD bouton formed a long symmetric synapse with the cell body at another level. Gold substitution. × 52 000.

Fig. 7. Parallel fibre varicosity (RV) forms asymmetric synapses with the soma of stellate cell no. 4 (at solid arrow) and with a dendritic spine (at open arrow). Gold substitution. × 27 500.

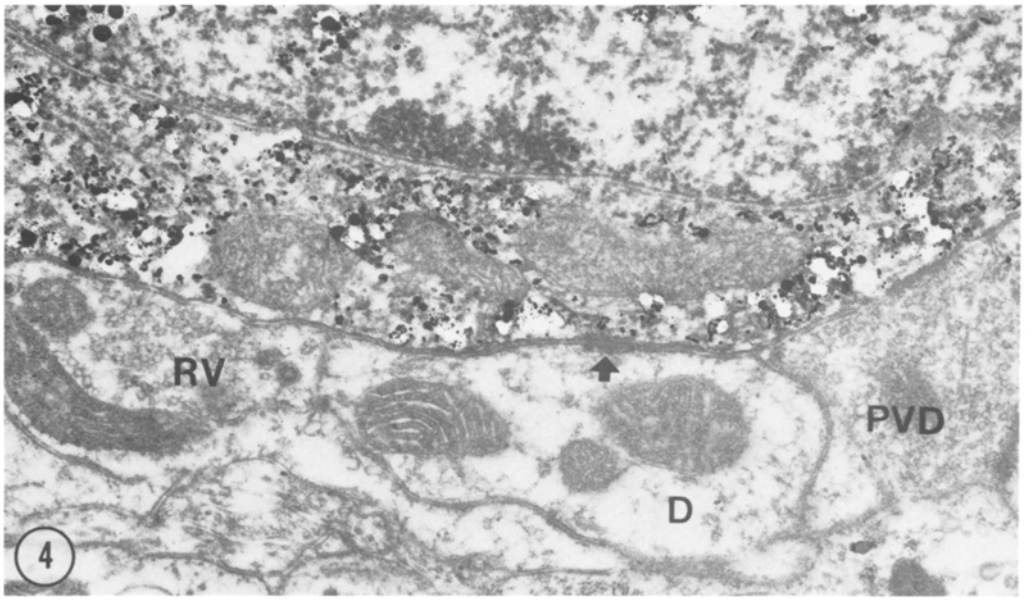
RV
PVD
D
4

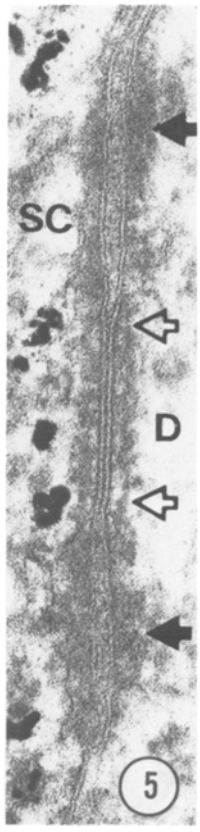
SC
D
5

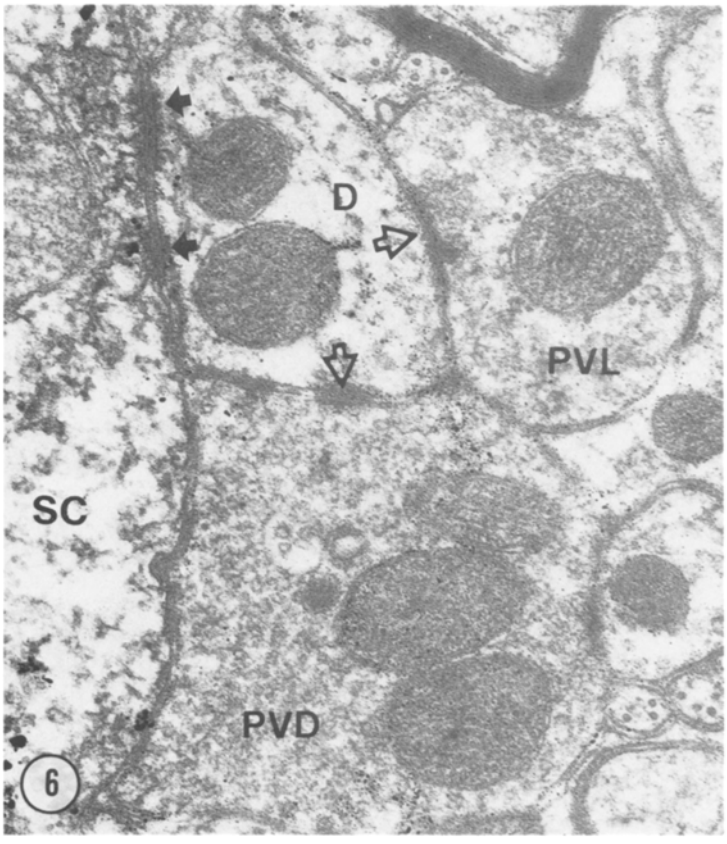
D
PVL
SC
PVD
6

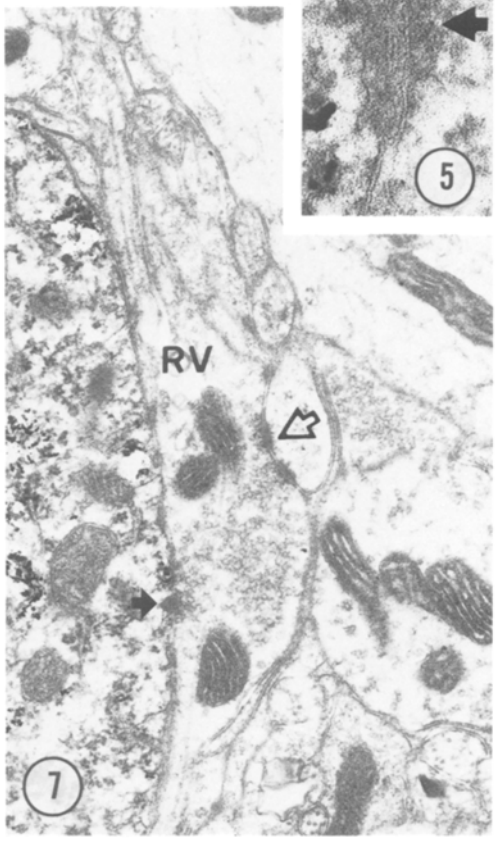
RV
7

stellate cells selected for electron microscopy (nos. 1, 4, 5 and 6, Fig. 1). The intial axon segments of cell nos. 1 and 6 are very thin (diameter decreasing rapidly in distal direction from 0.5 to 0.2 μm). They form no synaptic contacts and are surrounded by astrocytic profiles along the whole trajectory. Approximately 35 μm from the cell body they acquire a thin myelin shealth (5–10 lamellae); the axon diameters increase to about 0.5 μm and the impregation is gradually lost 5–10 μm from the beginning of the myelin sheath. The initial axon segments of cell nos. 4 and 6 are as thick as those of the other cells (0.5 μm) near the emanation cone, but they remain uniformly thick during their

---

Fig. 8. Primary dendrite (D_1) emerging from cell no. 7. An RV terminal and a dendro-dendritic apposition (open arrow) are indicated. Gold substitution. × 13 000.

Fig. 9. The dendro-dentritic apposition indicated in Fig. 8 is shown at high power. A gap junction (open arrow) and a punctum adhaerens (solid arrow) can be distinguished. × 65 000.

Fig. 10. Primary dendrite (D_1) of stellate cell no. 6. Note the irregular contour and the spines (open arrows). Two RV terminals forming asymmetric synapses on the dendritic shaft are indicated. RV_1 also contacts one of the spines. Gold substitution. × 24 000.

Fig. 11. The shaft of a secondary dendrite (D_2) of stellate cell no. 6 forms asymmetric synapses (open arrows) with three RV axon terminals. Gold substitution. × 19 000.

Fig. 12. Junction of the secondary dendrite (D_2) of stellate cell no. 7 and an unimpregnated small dendrite. The junction consists of two adjacent puncta adhaerentia (solid arrows). Gold substitution. × 38 000.

Fig. 13. Stellate cell no. 4 (SC) with the initial axon segment lying in the plane of section (arrowheads). Two nonimpregnated granule cells are labelled GC. Thin astrocytic sheaths surround the emerging stellate cell axon. Kodalith treatment. × 5900. Inset illustrates the axon of the same serially sectioned cell, at the point where it acquires a thin myelin sheath (arrowhead). × 17 500.

Fig. 14. Stellate cell no. 3 (SC) with the initial axon segment lying in the plane of section (arrowheads). No synapses are present on the emerging axon. The approximate sites where two parallel fibre varicosities came in contact with the cell body in neighbouring serial sections are indicated by open arrows. Gold substitution. × 9200. Inset illustrates the axon of the same serially sectioned cell, at the point where it acquires a thin myelin sheath (arrowhead). × 18 000.

Figs. 15–21 show electron micrographs from standard thin sections.

Figs. 15 and 16. These micrographs are enlargements of two small dendrites (1 and 2) in contact with the emerging dendrite of the stellate cell illustrated in Fig. 17. The two dendrites form similar junctional specializations. Gap junctions are marked by solid arrows and puncta adhaerentia by arrowheads. Postsynaptic densities facing boutons with RV boutons are indicated by open arrows. × 30 430.

Fig. 17. A stellate cell body with an emerging dendrite shows four apposed dendritic profiles (arabic numerals). The nucleus is indented and the cytoplasm contains numerous free polyribosomes. Note the contact with an unusually large PVL bouton and the two asymmetric synapses with RV boutons (open arrows). × 9200. The inset shows the associated punctum adhaerens and gap junction of $dendrite_1$. × 171 070.

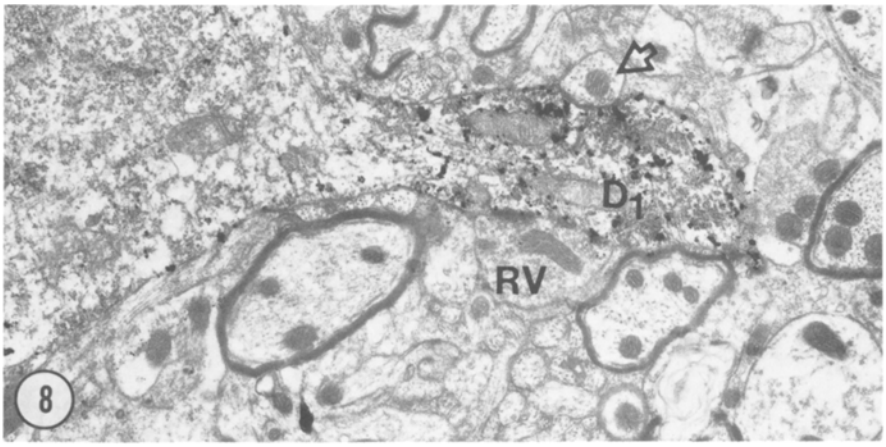

8

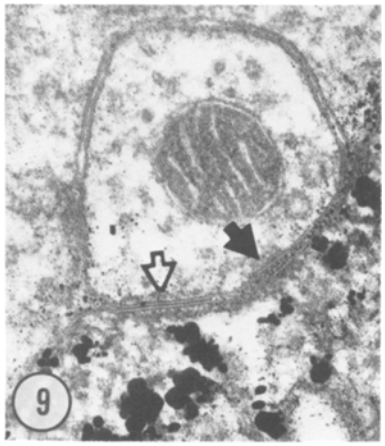

9

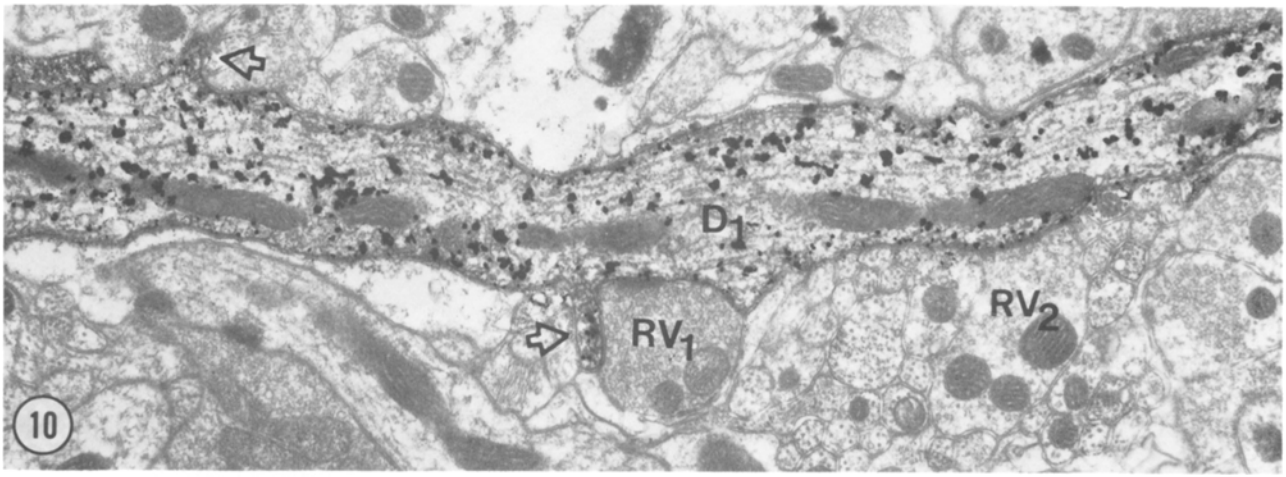

10

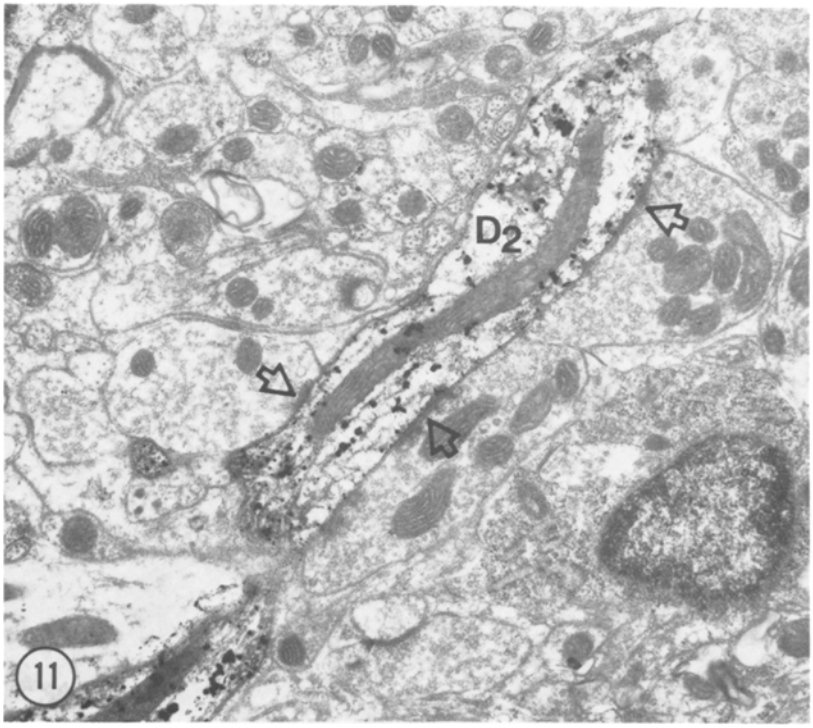

11

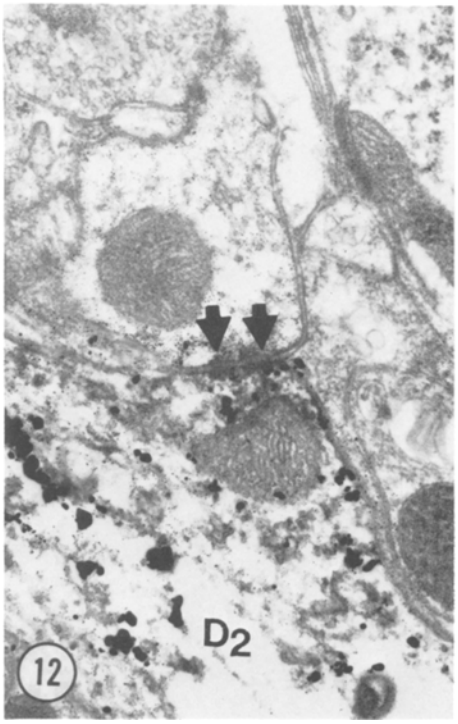

12

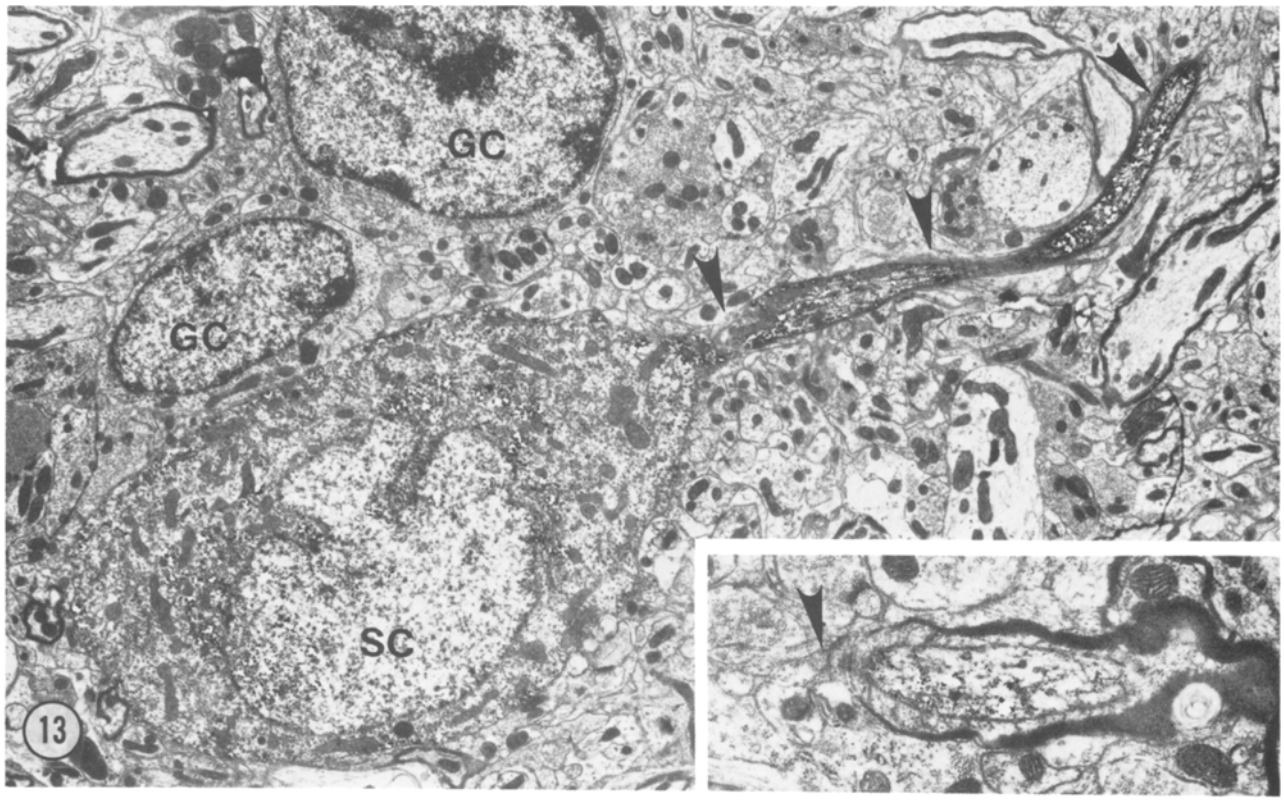
GC
GC
SC
13

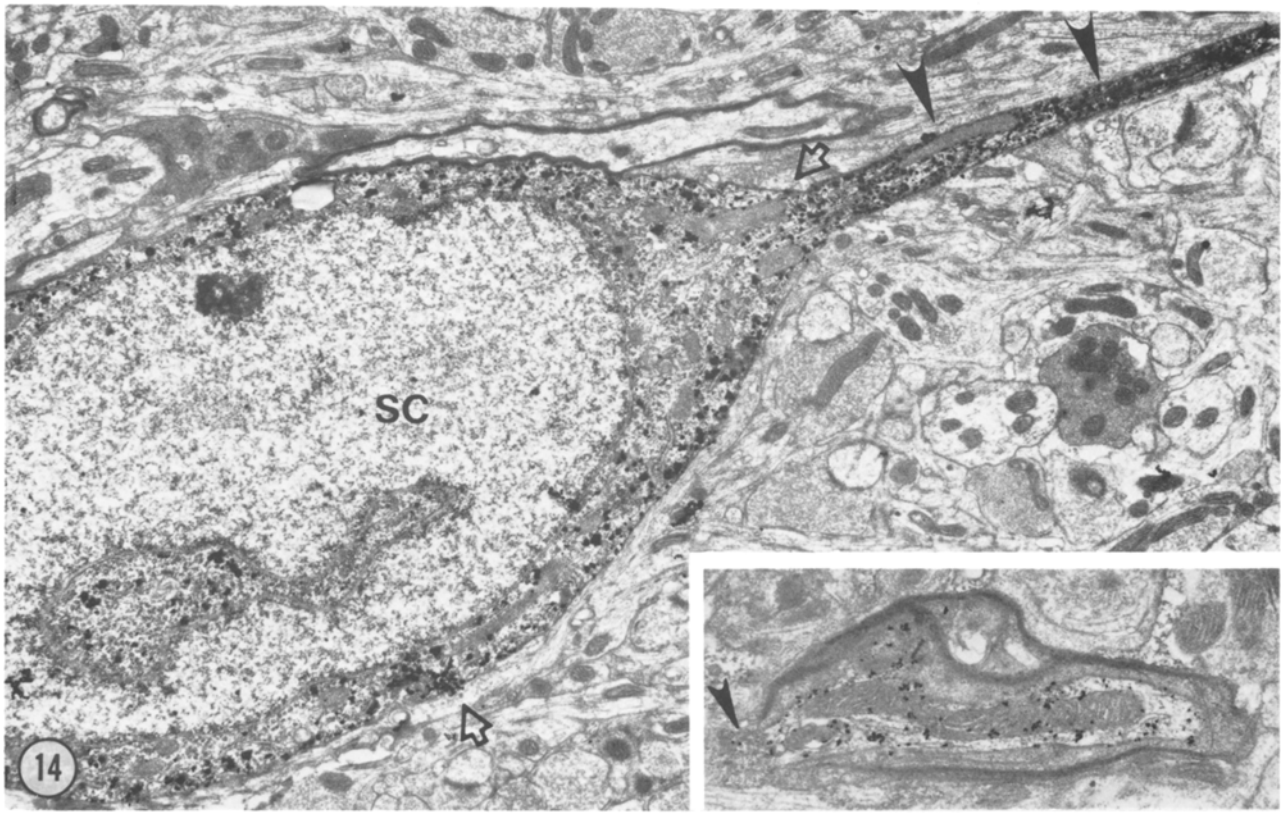
SC
14

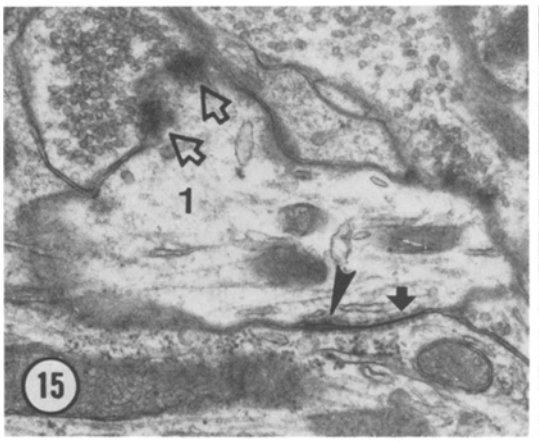

15

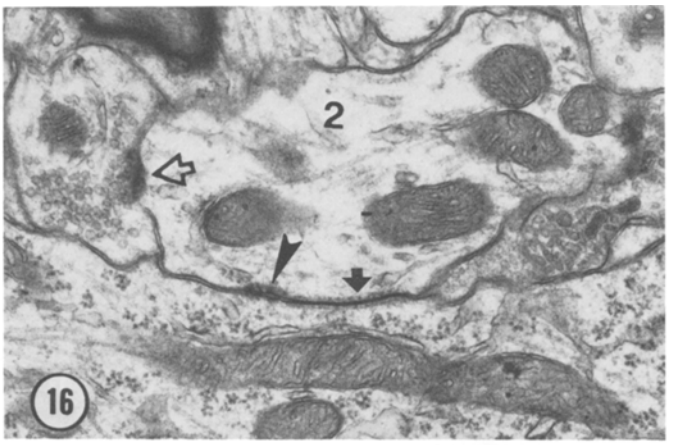

16

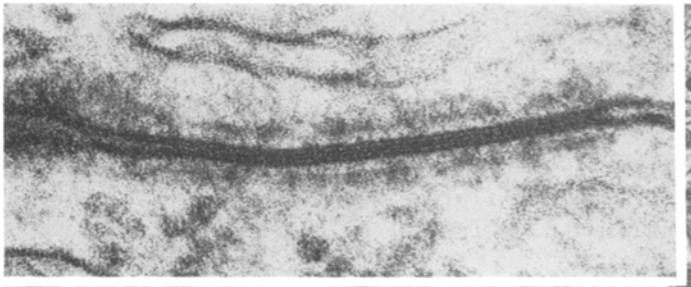

17

trajectory. They are also surrounded by astrocytic processes and acquire a thin myelin sheath (Figs. 13, 14, insets) after a trajectory of approximately 25 μm.

Identification of stellate cells in standard thin sections

The previous description of Golgi-impregnated cochlear stellate cells enabled us to identify putative neurons belonging to this class in standard thin sections of layers 1 and 2 of the DCN. Figs. 15–21 show such cells, their dendrites and synaptic contacts. The cell shown in Fig. 17 is located in the subependymal region of layer 1 and has a small diameter; the cell shown in Fig. 18 is located in the deep portion of layer 1 and is larger. Both cells are in contact with small dendrites. Gap junctions and/or puncta adhaerentia are seen at most of these dendro-somatic appositions. Synapses of parallel fibres on layer 1 stellate cells are shown in Figs. 19 and 20. Some of the parallel fibres have a thin myelin sheath (Fig. 20), which they lose near a synaptic varicosity.

A thin dendrite with parallel fibre synapses on the shaft is shown in Fig. 21. Such dendrites are seen in both layers 1 and 2. They have few pleomorphic spines and often form dendro-dendritic appositions featuring puncta adhaerentia and gap junctions like the Golgi-impregnated stellate cell dendrites. In the standard thin section the intercellular cleft of the gap junction usually measures 2 nm (inset to Fig. 17) and the points of occlusion observed in the Golgi-impregnated thin sections are lacking. Such thin dendrites are easily distinguished from the spiny cartwheel cell dentrites (d_2 in Fig. 21) (Wouterlood & Mugnaini, 1984), the spiny pyramidal cell dendrites (Kane, 1974a) and the hairy Golgi cell dendrites (Mugnaini *et al.*, 1980a).

Discussion

LIGHT MICROSCOPY

Stellate cells resembling those observed in this study have been described previously in the outer two layers of DCN in various mammals by Cajal (1911; 'cellules de la couche plexiforme'; cat), Lorente de Nó (1933, 1979, 1981a; 'type B or star cells'; mouse and cat), Cohen (1972; 'small spherical cells'; cat), Brawer *et al.* (1974; 'small stellate neurons'; cat), Disterhoft *et al.* (1980; 'small stellate cells'; rabbit), Osen & Mugnaini (1981; 'stellate cells'; rat, guinea-pig and cat), Browner & Baruch (1982; 'small spherical neurons'; mouse), and Webster & Trune (1982; 'longitudinal and horizontal small neurons'; mouse). Most stellate cells are larger than granule cells and smaller than the other small neurons of the DCN. The range of cell body sizes of the stellate neurons (9–14 μm),

---

Fig. 18. The largest stellate cell in our sample shows four dendro-somatic contacts (arabic numerals). Two large cytoplasmic regions (asterisks) contain a high density of free polyribosomes and some cisterns of the granular endoplasmic reticulum. IAS marks the emerging axons surrounded by astrocytic processes. Arrow points to a symmetric synapse with a PVD bouton. × 9700.

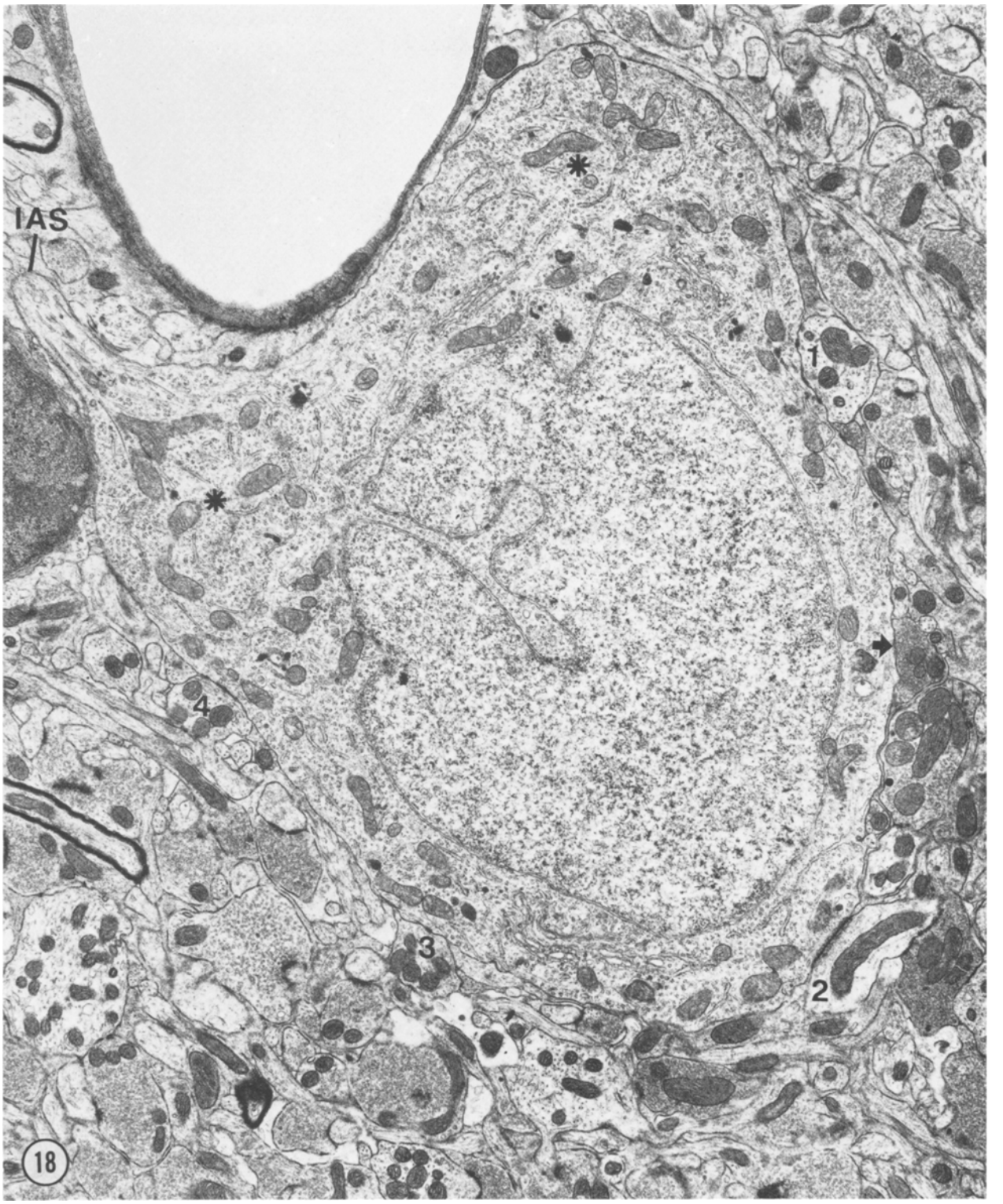
IAS
1
2
3
4
18

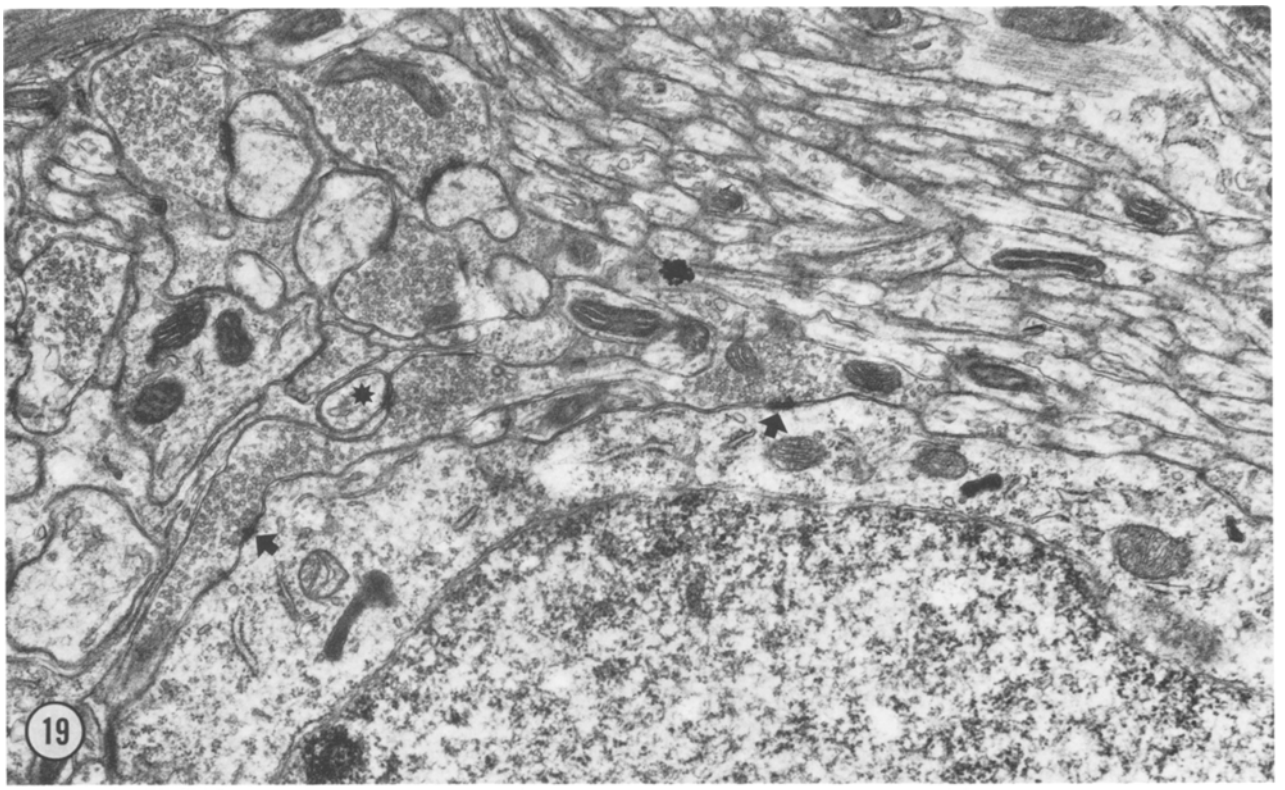
19

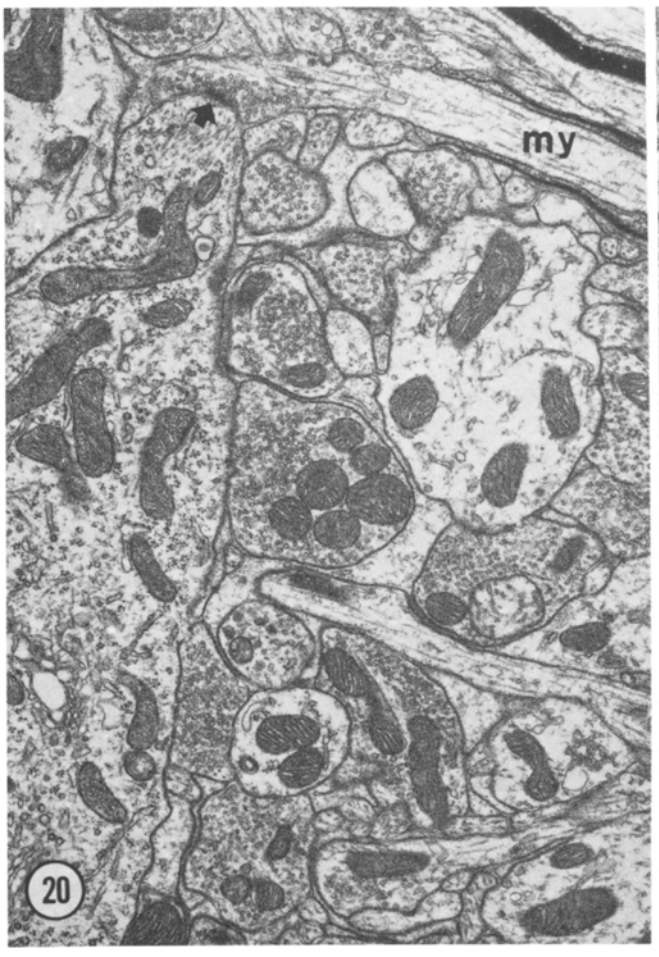
my
20


d1
d2
21

however, overlaps at either end of the spectrum with that of granule cells (6–9 μm) and cartwheel cells (10–14 μm), the most frequently occurring neurons in the outer two DCN layers (Wouterlood & Mugnaini, 1984).

All authors agree that the dendrites of these three types of neuron have distinctive features. As verified electron microscopically, granule cell dendrites are short, with terminal claws (Mugnaini *et al.*, 1980,a,b), and cartwheel dendrites are curved and studded with spines (Wouterlood & Mugnaini, 1984). The granule-associated cochlear Golgi cells, described by Mugnaini *et al.* (1981a), occur not only in layers 1 and 2 of the DCN, but also in the granule cell domain of the ventral cochlear nucleus. They resemble somewhat stellate cells in body size and dendritic pattern. Their hair somatic appendages and tapering main stem dendrites, however, make them distinguishable from the stellate cells analysed in this study.

Dendrites of granule and Golgi cells enter glomeruli and receive synapses from mossy fibres, some of which originate in the brain stem (Kane & Finn, 1977). Granule cell axons form parallel fibres which occupy a large volume of layer 1. They are presumably excitatory and use glutamate or aspartate as neurotransmitter (Oliver *et al.*, 1983). Parallel fibres contact not only the stellate cells but also the apical dendrites of pyramidal cells and the cartwheel cell dendrites (Kane, 1974a, b; Mugnaini *et al.*, 1980b; Wouterlood & Mugnaini, 1984). Golgi cells are thought to be inhibitory; their axons feed back onto granule cells (Mugnaini *et al.*, 1980b). Cartwheel cells (type C cells of Lorente de Nó, 1981a) have myelinated axons that branch within the DCN. It has been suggested that they are inhibitory interneurons somewhat similar to cerebellar Purkinje cells (Wouterlood & Mugnaini, 1984).

Morphological clues concerning the function of stellate cells can be obtained by transmitter immunocytochemistry and by identification of their axon terminals. The cell bodies of stellate neurons, like those of cartwheel neurons, are immunolabelled with an antiserum against glutamate decarboxylase, the biosynthetic enzyme for the inhibitory neurotransmitter GABA (unpublished observations). The axons of stellate cells are always impregnated only for a short distance in adult rats. This feature suggests that they acquire a myelin sheath, as confirmed by electron microscopy. Lorente de Nó (1933,

---

Fig. 19. The soma of a subependymal stellate cell receives two asymmetric synapses (arrows) from *en passant* varicosities of the same parallel fibre. This fibre also forms a synapse with a dendritic spine (asterisk). × 21 800.

Fig. 20. A thin myelinated fibre (my), oriented parallel to the long axis of the DCN, loses the myelin sheath and forms a synapse (arrow) with the emerging dendrite of a stellate cell. The synaptic vesicles in the varicosity are round. × 15 900.

Fig. 21. The shaft of a thin dendrite (d_1) forms asymmetric synapses (solid arrows) with varicosities of parallel fibres that contain round synaptic vesicles, and symmetric synapses (arrowheads) with boutons containing pleomorphic vesicles. A nearby cross-sectioned dendrite (d_2), surrounded by globular spines (asterisks), is interpreted as a second-order branch belonging to a cartwheel neuron (see Wouterlood & Mugnaini, 1984). The thin dendrite (d_1) forms a thin spine provided with a large triangular base (open arrow). × 12 900.

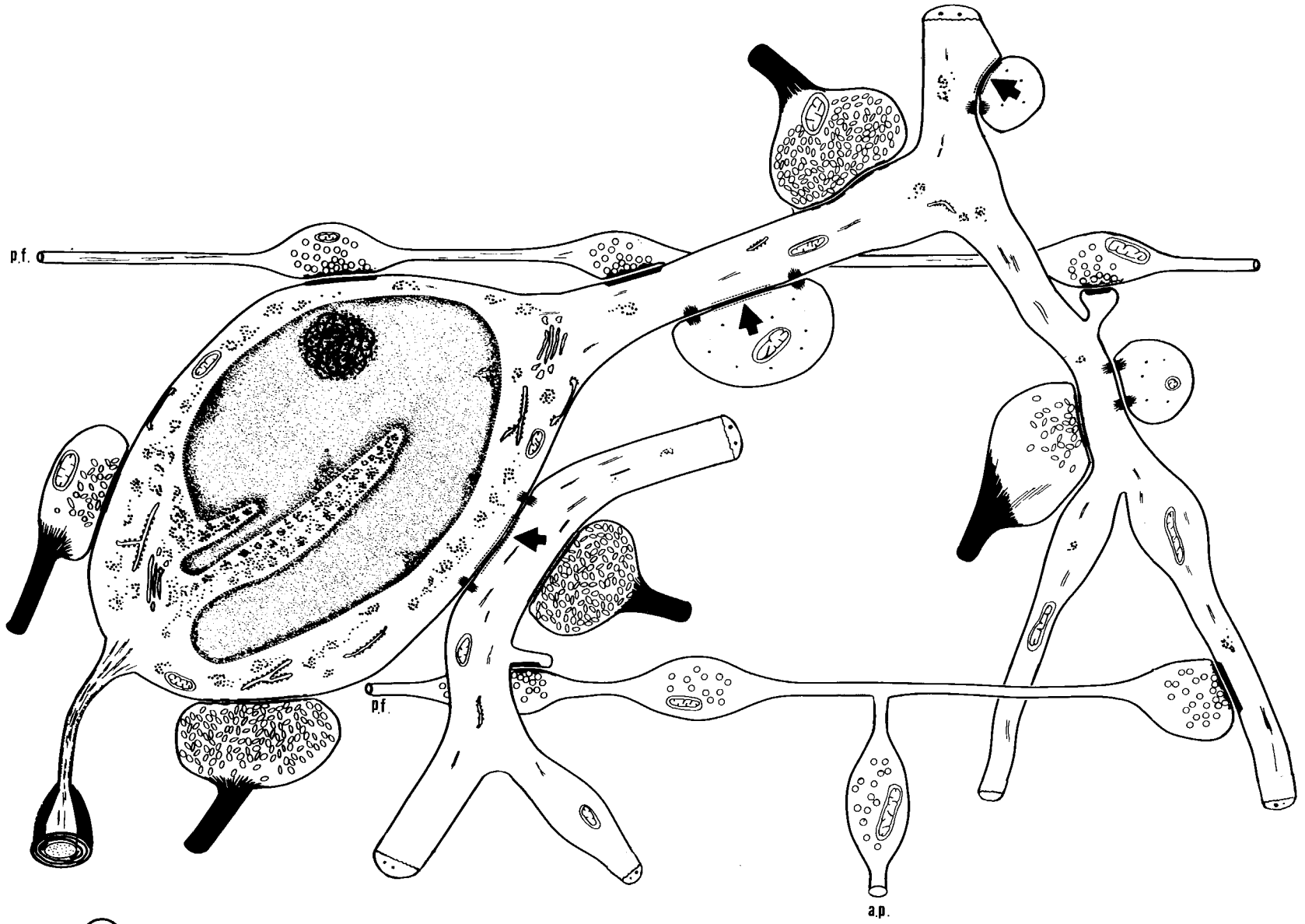

22

1981a) observed many DCN stellate cells with impregnated axons in young mice and in kittens. The axons branched profusely and remained within the outer two layers. We therefore consider the stellate cells of the outer two DCN layers as inhibitory local circuit neurons. Stellate cells with myelinated axons are not features unique of the DCN; they have been observed also in the cerebral cortex (Peters & Proskauer, 1980; Lorente de Nó, 1981b).

ELECTRON MICROSCOPY

Cell body, dendrites and chemical synapses

In electron micrographs of Golgi-impregnated stellate cells from layer 1 we observed a set of distinctive ultrastructural features (diagrammatically represented in Fig. 22) which afford identification of many of these neurons in standard ultrathin sections. As reported elsewhere (Wouterlood & Mugnaini, 1984), a rough estimate based on standard thin sections shows that stellate cells are relatively more numerous in layer 2 than in layer 1. The stellate cells occur more frequently than Golgi cells, but are outnumbered by both granule cells and cartwheel neurons. Stellate perikarya have a larger nucleus to cytoplasm ratio than cartwheel cells. The nucleus is indented and the chromatin, evenly dispersed in the nuclear interior, forms small dense clumps along the nuclear envelope. In the cytoplasm, short and long cisterns of the granular endoplasmic reticulum (ER) are present in all sections, but stacked cisterns of granular ER are rare. The cells contain one or two cytoplasmic zones particularly rich in free polyribosomes with interspersed granular cisterns, which in Nissl sections may appear as Nissl bodies. Unlike cartwheel cells (Wouterlood & Mugnaini, 1984) and pyramidal cells (Fiori & Mugnaini, 1981), stellate cells infrequently show mitochondria associated with subsurface cisterns. Furthermore, the stellate cells never show the multiple assemblies of mitochondria and flattened cisterns characteristic of cartwheel cells (Wouterlood & Mugnaini, 1984). Golgi cells, which lack both these assemblies and the dendro-somatic gap junctions, usually have several somatic appendages and may form synapses with large mossy terminals.

The cell body and the dendritic shafts of stellate cells receive both asymmetric and symmetric synapses. Asymmetric synapses are formed with boutons, presumed to be

Fig. 22. Diagrammatic representation of the salient features of stellate cells in layers 1–2 of the rat DCN. The relatively large nucleus is indented and has a thin peripheral rim of heterochromatin. The cytoplasm contains numerous free polyribosomes and the granular ER consists of individual cisterns. The thin dendrites arise abruptly from the cell body and bear few spines which lack a spine apparatus. The axon acquires a thin myelin sheath. Asymmetric synapses on the cell body, dendritic shafts and spines are formed with varicosities containing round synaptic vesicles which are interpreted as parallel fibre portions (pf) and ascending portions (ap) of granule cell axons. Symmetric synapses are formed on the cell body and the dendritic shafts with two kinds of boutons (represented with darkened stems) containing pleomorphic vesicles. The soma and the dendrites form gap junctions (arrows) with thin dendrites, most of which presumably belong to neighbouring stellate cells.

p.f.
p.f.
p.f.
p.f.
p.f.
p.f.
1
2
3
4
5
6
7
8
9
a
EPENDYMA
LAYER 1
LAYER 2
LAYER 3

excitatory, that contain round synaptic vesicles and represent *en passant* varicosities of thin fibres interpreted as granule cell axons (either their ascending portions or their terminal parallel fibres). These varicosties also form asymmetric synapses with the spiny dendritic branches of the cartwheel cells (Wouterlood & Mugnaini, 1984) and the apical pyramidal cell arbors (Kane, 1974a; and our upublished observations) but they do not synapse with the cell bodies of such neurons. Symmetric synapses on stellate cells are formed with at least two kinds of bouton, presumed to be inhibitory, containing pleomorphic synaptic vesicles (PVD and PVL boutons). These boutons, also found on the cell bodies and dendritic shafts of cartwheel cells (Wouterlood & Mugaini, 1984) and on pyramidal cells (Kane, 1974a; and our unpublished observations), arise from fibres running in various directions. Some of these fibres contain numerous neurofilaments. Immunoelectron microscopic studies in progress in our laboratories indicate that numerous boutons with pleomorphic synaptic vesicles in the outer two layers of the DCN contain glutamic acid decarboxylase (GAD), and, therefore, may use GABA as a transmitter. Although we believe than many of the boutons with pleomorphic synaptic vesicles in layers 1 and 2 represent terminals of the locally branching stellate and cartwheel cell axons, it is possible that some of them originate from neurons situated outside the DCN.

Gap junctions

Dendro-somatic and dendro-dendritic contacts occur frequently on stellate cells. Such contacts show a gap junction accompanied by puncta adhaerentia, an association of cell junctions noted on many types of vertebrate neuron (Pappas & Waxman, 1972; Sotelo & Llinás, 1972; Peters *et al.*, 1976). Most of the dendrites forming gap junctions with the perikarya and dendrites of Golgi-impregnated stellate cells resemble typical stellate dendrites. We assume, therefore, that stellate cells are extensively coupled with each other by gap junctions, although we cannot exclude that dendrites of other neurons participate in these associations. Dendro-dendritic and dendro-somatic gap junctions in the rat cochlear nuclei have been described by Sotelo *et al.* (1976); Their observations, however, concerned another type of neuron located in the ventral cochlear nucleus. Thus, our observation of gap junctions between stellate cells in layers 1 and 2 of the DCN is a new finding. In addition, in the course of our studies on the DCN we have observed puncta adhaerentia and occasional gap junctions between dendrites in layer 1 that differ from stellate cell dendrites.

Fig. 23. Tentative, diagrammatic representation of the circuit in the DCN involving the stellate cells (solid black, labelled 1–3). The stellate cells form dendro-dendritic and dendro-somatic gap junctions with one another (arrows). Excitatory input is mainly provided by parallel fibres, the axons of granule cells (white, labelled 6–8). Granule cell activity is modulated by associated interneurons termed cochlear Golgi cells (dotted black, labelled 9). Based on neonatal Golgi sections, it is assumed that the thinly myelinated stellate cell axons arborize in layers 1–2 (dashed lines) and form synapses with stellate cells, with cartwheel cells (dotted black, labelled 5), and with pyramidal cells (principal neuron, white labelled 4). The initial axon segments are indicated by *a*.

STELLATE CELLS IN DCN AND IN CEREBELLAR CORTEX

The stellate cells in the outer two layers of the DCN resemble stellate cells in the cerebellar cortex (Eccles *et al.*, 1967; Sotelo & Llinás, 1972; Mugnaini, 1972; Palay & Chan-Palay, 1974) with regard to their axo-somatic and axo-dendritic synapses and the fine structure of cell bodies and dendrites. Both cell types are coupled by gap junctions and receive asymmetric synapses from the axons of granule cells, largely in the form of parallel fibre varicosities. These synapses are located not only on dendritic spines, but also on dendritic shafts and cell bodies. The dendrites arise abruptly from the cell bodies and bear few spines. The cell bodies vary in size according to a positional gradient. As discussed by Cajal (1911), Lemkey-Johnston & Larramendi (1968), Larramendi (1969), Mugnaini (1969) and Rakic (1972), the appositional growth in the cerebellar molecular layer indicates that the expression of different sizes by stellate cells is related to their time of origin. Presumably, a similar growth pattern is present in the DCN (Altman & Das, 1966; Pierce, 1967; Altman & Bayer, 1980).

Differences in the stellate cells of the two regions, however, should also be noted. Whereas in the cerebellar cortex the stellate cell dendrites have a nearly monoplanar configuration with their dendritic arbor across the parallel fibres, the DCN stellate cell dendrites extend in all directions. Furthermore, axons of cerebellar stellate cells are unmyelinated, whereas those of DCN stellate cells are provided with thin myelin sheaths.

The correlation of gap junctions and electrotonic coupling has been established in different neurons in a large variety of animals (Bennett, 1977). One can assume, therefore, that the stellate cells in the DCN and cerebellar molecular layers are coupled electrotonically. Since the neuronal circuitries in the DCN and cerebellar molecular layers display similarities, one may surmise that cochlear and cerebellar stellate cells have analogous functions, i.e. they are activated mainly by parallel fibres, and provide feedforward inhibition to other stellate cells and to the spiny neurons as shown schematically in Fig. 23. The functional significance of the gap junctional connectivity in these layers may be 'entrenchment'. Analogy with other electrotonically coupled systems (Bennett, 1977) suggests that mutual coupling between stellate cells would tend to make their firing synchronous or close to synchronous. The advantages of such a synchronization would be that of increasing inhibitory effectiveness with increased input size (Llinas, personal communication). Interestingly, [^{14}C]2-deoxyglucose studies indicate that the DCN has a high level of resting activity (Schwartz & Sharp, 1978; Jones & Disterhoft, 1979; Nudo & Masterton, 1981). Stellate cells of layers 1 and 2 of the DCN, therefore, might fire synchronously at low levels of sound stimulation.

GENERAL CONSIDERATIONS

Coupling by gap junctions of inhibitory local circuit neurons is not restricted to the DCN and cerebellum, but also has been observed in other laminated grey matters. In the retina of monkeys and rabbits, gap junctions occur between horizontal cells in the outer plexiform layer (Raviola & Gilula, 1975). In the primate sensori-motor cortex,

dendro-dendritic and dendro-somatic gap junctions (Sloper, 1972; Sloper & Powell, 1978a) occur between large stellate cells of the deep layers, which correspond to the cortical basket cells of light microscopy (Marin-Padilla, 1969), a type of GABAergic local circuit neuron (Ribak, 1978). They also occur between presynaptic dendrities. These are provided with pleomorphic vesicles, form symmetric synaptic junctions, and presumably belong to another kind of inhibitory stellate cell (Sloper & Powell, 1978b). Dendro-dendritic gap junctions have also been observed in the rat visual cortex (Peters, 1980). Although in all these regions the gap junctions make up a small percentage of all synaptic contacts in the neuropil, their importance for the coupled cells in particular could be substantial. Electrotonic coupling with dendro-dendritic and dendro-somatic gap junctions, although a feature scarcely appreciated so far when considering general principles of neural organization, could represent one of the basic modes of circuit designs involving inhibitory local circuit neurons in laminated grey matters.

Acknowledgements

This work was supported by US-PHS grant NS 09904. We are greatly indebted to the Niels Stensen Stiching of Amsterdam, The Netherlands, for a visiting fellowship to Dr F. G. Wouterlood and to the Norwegian Research Council for Science and the Humanities and The Norwegian Academy for Science and Letters for a visiting fellowship to Dr K. K. Osen.

References

ADAMS, J. C. (1979) A fast, reliable silver-chromate Golgi method for perfusion-fixed tissue. *Stain Technology* **54**, 225–6.

ALTMAN, J. & BAYER, S. A. (1980) Development of the brain stem in the rat. III. Thymidine-radiographic study of the time of origin of neurons of the vestibular and auditory nuclei of the upper medulla. *Journal of Comparative Neurology* **194**, 877–904.

ALTMAN, J. & DAS, G. (1966) Autoradiogrpahic and histological studies of postnatal histogenesis. II. A longitudinal investigation of kinetics, migration and transformation of cells incorporating thymidine in infant rats with special reference to postnatal neurogenesis in some brain regions. *Journal of Comparative Neurology* **126**, 337–90.

BENNETT, M. V. L. (1977) Electrical transmission: a functional analysis and comparison with chemical transmission. In: *Cellular Biology of Neurons* (edited by KANDEL, E. R.), Handbook of Physiology – The Nervous System, Vol. 1, pp. 357–416. Baltimore: Williams and Wilkins.

BLACKSTAD, T. W., OSEN, K. K. & MUGNAINI, E. (1984) Pyramidal neurons of the dorsal cochlear nucleus: a Golgi and computer reconstruction study in the cat. *Neuroscience* (in press).

BRAWER, R. J., MOREST, D. K. & KANE, E. C. (1974) The neuronal architecture of the cochlear nucleus of the cat. *Journal of Comparative Neurology* **155**, 251–300.

BRODAL, A. (1981) The auditory system (revised by K. K. Osen). In *Neurological Anatomy* (edited by BRODAL, A.), pp. 692–739. Oxford: Oxford University Press.

BROWNER, R. H. & BARUCH, A. (1982) The cytoarchitecture of the dorsal cochlear nucleus in the 3-month- and 26-month-old C57B1/6 mouse. A Golgi impregnation study. *Journal of Comparative Neurology* **211**, 115–38.

CAJAL, S. R. Y. (1911) *Histologie du Système Nerveux de l'Homme et des Vertébrés*, Vol. I. Paris: Maloine.

COHEN, E. (1972) The synaptic organization of the caudal cochlear nucleus in the cat: a light and electron microscopical study. *Doctoral Dissertation*. Harvard University, Cambridge.

COLONNIER, M. (1968) Synaptic patterns on different cell types in different laminae of the cat visual cortex. An electron microscopic study. *Brain Research* **9**, 268–87.

DISTERHOFT, J. F., PERKINS, R. E. & EVANS, S. (1980) Neuronal morphology of the rabbit cochlear nucleus. *Journal of Comparative Neurology* **192**, 687–702.

ECCLES, J. C., ITO, M. & SZENTÁGOTHAI, J. (1967) *The Cerebellum as a Neuronal Machine*. Berlin: Springer-Verlag.

FAIRÉN, A., DeFELIPE, J. & MARTINEZ-RUIZ, R. (1981) The Golgi-EM procedure: a tool to study neocortical interneurons. In: *Glial and Neuronal Cell Biology*, Progress in Clinical and Biological Research, Vol. 59A (edited by ACOSTA VIDRIO, E. and FEDOROFF, S.), pp. 219–301. New York: Alan R. Liss.

FAIRÉN, A., PETERS, A. & SALDANHA, J. (1977) A new procedure for examining Golgi-impregnated neurons by light and electron microscopy. *Journal of Neurocytology* **6**, 311–37.

FIORI, M. G. & MUGNAINI, E. (1981) Subsurface and cytoplasmic cisterns associated with mitochondria in pyramidal neurons of the rat dorsal cochlear nucleus. *Neuroscience* **6**, 461–71.

FRIEDRICH, V. L. JR, & MUGNAINI, E. (1981) Electron microscopy: preparation of neural tissues for electron microscopy. In: *Neuroanatomical Tract-Tracing Methods* (edited by HEIMER, L. and ROBARDS, M. J.), pp. 345–376. New York: Plenum Press.

GRAY, E. G. (1959) Axosomatic and axodendritic synapses of the cerebral cortex. *Journal of Anatomy* **93**, 420–33.

JONES, L. S. & DISTERHOFT, J. F. (1979) Visualizing the rabbit auditory pathway with (^{14}C)-2-deoxy-D-glucose. *Society for Neuroscience Abstracts* **5**, 23.

KANE, E. C. (1974a) Synaptic organization in the dorsal cochlear nucleus of the cat: a light and electron microscopic study. *Journal of Comparative Neurology* **155**, 301–30.

KANE, E. C. (1974b) Patterns of degeneration in the caudal cochlear nucleus of the cat after cochlear ablation. *Anatomical Record* **179**, 67–92.

KANE, E. C. & FINN, R. C. (1977) Descending and intrinsic inputs to dorsal cochlear nucleus of cats: a horseradish peroxidase study. *Neuroscience* **2**, 897–912.

LARRAMENDI, L. M. H. (1969) Analysis of synaptogenesis in the cerebellum of the mouse. In: *Neurobiology of Cerebellar Evolution and Development* (edited by LLINÁS, R.) pp. 803–843. Chicago: AMA-ERF Institute for Biomedical Reserach.

LEMKEY-JOHNSTON, N. & LARAMENDI, L. M. H. (1968) Types and distribution of synapses upon basket and stellate cells of the mouse cerebellum: an electron microscopic study. *Journal of Comparative Neurology* **134**, 73–112.

LORENTE DE NÓ, R. (1933) Anatomy of the eighth nerve. III. General plan of structure of the primary cochlear nuclei. *Laryngoscope* **43**, 327–50.

LORENTE DE NÓ, R. (1979) Central representation of the eighth nerve. In *Ear Diseases, Deafness and Dizziness* (edited by GOODHILL, V.), pp. 64–86. Hagerstown, Maryland: Harper & Row.

LORENTE DE NÓ, R. (1981a) *The Primary Acoustic Nuclei*, pp. 1–177. New York: Raven Press.

LORENTE DE NÓ, R. (1981b) Neurons with short axons in the adult human visual cortex. *Freiburger Universitatsblatter* **74**, 59–61.

MARIN-PADILLA, M. (1969) Origin of pericullular baskets of the human motor cortex: a Golgi study. *Brain Research* **14**, 633–46.

MUGNAINI, E. (1969) Ultrastructural studies on the cerebellar histogenesis. II. Maturation of nerve cell populations and establishment of synaptic connections in the cerebellar cortex of the chick. In: *Neurobiology of Cerebellar Evolution and Development* (edited by LLINÁS, R.), pp. 749–782. Chicago: AMA-ERF Institute for Biomedical Research.

MUGNAINI, E. (1972) The histology and cytology of the cerebellar cortex. In: *The Comparative Anatomy and Histology of the Cerebellum: The Human Cerebellum, Cerebellar Connections and Cerebellar Cortex* (edited by LARSELL, O. and JANSEN, J.), pp. 201–265. Minneapolis: University of Minnesota Press.

MUGNAINI, E., OSEN, K. K., DAHL, A.-L., FREIDRICH, V. L. JR & KORTE, G. (1980a) Fine structure of granule cells and related interneurons (termed Golgi cells) in the cochlear nuclear complex of cat, rat and mouse. *Journal of Neurocytology* **9**, 537–70.

MUGNAINI, E., WARR, W. B. & OSEN, K. K. (1980b) Distribution and light microscope features of granule cells in the cochlear nuclei of cat, rat and mouse. *Journal of Comparative Neurology* **191**, 581–606.

NUDO, R. J. & MASTERTON, R. B. (1981) (^{14}C)-2-deoxyglucose mapping of the dorsal cochlear nucleus in the kitten. *Society for Neuroscience Abstracts* **7**, 230.

OLIVER, D. L., POTASHNER, S. J., JONES, D. R. & MOREST, D. K. (1983) Selective labelling of spiral ganglion and granule cells with D-aspartate in the auditory system of cat and guinea pig. *Journal of Neuroscience* **3**, 455–72.

OSEN, K. K. & MUGNAINI, E. (1981) Neuronal circuits in the dorsal cochlear nucleus. In: *Neuronal Mechanisms of Hearing* (edited by SYKA, J. and AITKIN, L.). pp. 119–126. New York: Plenum Press.

PALAY, S. L. & CHAN-PALAY, V. (1974) *Cerebellar Cortex. Cytology and Organization*, pp. 1–348. New York: Springer-Verlag.

PAPPAS, G. D. & WAXMAN, S. G. (1972) Synaptic fine structure: morphological correlations of chemical and electronic transmission. In: *Structure and Function of Synapses* (edited by PAPPAS, G. D. and PURPURA, D. P.), pp. 1–43. New York: Raven Press.

PETERS, A. (1980) Morphological correlates of epilepsy: cells in the cerebral cortex. In: *Antiepileptic Drugs. Mechanisms of Action* (edited by GLASER, G. H., TENZY, J. K. and WOODBURY, D. N.), pp. 21–48. New York: Raven Press.

PETERS, A., PALAY, S. L. & WEBSTER, H. deF. (1976) *The Fine Structure of the Nervous System*, pp. 1–406. Philadelphia: Saunders.

PETERS, A. & PROSKAUER, C. C. (1980) Synaptic relationships between a multipolar stellate cell and a pyramidal neuron in the rat visual cortex. A combined Golgi–electron microscopic study. *Journal of Neurocytology* **9**, 185–205.

PIERCE, E. T. (1967) Histogenesis of the dorsal and ventral cochlear nuclei in the mouse. An autoradiographic study. *Journal of Comparative Neurology* **131**, 27–54.

RAKIC, P. (1972) Extrinsic cytological determinants of basket and stellate cell dendritic pattern in the cerebellar molecular layer. *Journal of Comparative Neurology* **146**, 335–54.

RAVIOLA, E. & GILULA, N. B. (1975) Intramembrane organization of specialized contacts in the outer plexiform layer of the retina. A freeze-fracture study in monkeys and rabbits. *Journal of Cell Biology* **65**, 192–222.

RHODE, W. S., SMITH, P. H. & OERTEL, D. (1983) Physiological response properties of cells labeled intracellularly with horseradish peroxidase in cat dorsal cochlear nucleus. *Journal of Comparative Neurology* **213**, 426–47.

RIBAK, C. E. (1978) Aspinous and sparsely-spinous stellate neurons in the visual cortex of rats contain glutamic acid decarboxylase. *Journal of Neurocytology* **7**, 461–78.

SCHWARTZ, W. J. & SHARP, F. R. (1978) Autoradiographic maps of regional brain glucose consumption in resting, awake rats using (^{14}C)-2-deoxy-glucose. *Journal of Comparative Neurology* **177**, 335–60.

SLOPER, J. J. (1972) Gap junctions between dendrites in the primate cortex. *Brain Research* **44**, 641–6.

SLOPER, J. J. & POWELL, T. P. S. (1978a) Dendro-dendritic and reciprocal synapses in the primate motor cortex. *Proceedings of the Royal Society of London, Series B* **203**, 23–38.

SLOPER, J. J. & POWELL, T. P. S. (1978b) Gap junctions between dendrities and somata of neurons in the primate sensori-motor cortex. *Proceedings of the Royal Society of London, Series B* **203**, 39–47.

SOTELO, C., GENTSCHEV, T. & ZAMORA, A. J. (1976) Gap junctions in the ventral cochlear nucleus of the rat. A new example of electronic junctions in the mammalian CNS. *Neuroscience* **1**, 5–7.

SOTELO, C. & LLINÁS, R. (1972) Specialized membrane junctions between neurons in the vertebrate cerebellar cortex. *Journal of Cell Biology* **53**, 271–89.

WEBSTER, D. B. & TRUNE, D. R. (1982) Cochlear nucleus complex of mice. *American Journal of Anatomy* **163**, 103–30.

WILLARD, F. H. & RYUGO, D. K. (1983) Anatomy of the central auditory system. In: *The Auditory Psychobiology of the Mouse* (edited by WILLOT, J. F.), pp. 201–304. Springfield, Illinois: Thomas.

WOUTERLOOD, F. G. (1979) Light microscopical identification of Golgi impregnated CNS neurons during sectioning for electron microscopy. *Stain Technology* **54**, 325–9.

WOUTERLOOD, F. G. & MUGNAINI, E. (1984) Cartwheel neurons of the dorsal cochlear nucleus. A Golgi-electron microscopic study in rat. *Journal of Comparative Neurology* (in press).

WOUTERLOOD, F. G., NEDERLOF, J. & PANIRY, S. (1983) Chemical reduction of silver chromate: a procedure for electron microscopical analysis of Golgi-impregnated neurons. *Journal of Neuroscience Methods* **7**, 295–308.